Journal of Alloys and Compounds 504S (2010) S439–S442

Contents lists available at ScienceDirect

Journal of Alloys and Compounds

journal homepage: www.elsevier.com/locate/jallcom

Enhanced ductility of high-strength electrodeposited nanocrystalline Ni–Co alloy with fine grain size

Liyuan Qin, Jianshe Lian*, Qing Jiang

Key Lab of Automobile Materials, Ministry of Education, College of Materials Science and Engineering, Jilin University, Nanling campus, Changchun, 130025, China

ARTICLE INFO

Article history:
Received 29 June 2009
Received in revised form 14 February 2010
Accepted 21 February 2010
Available online 3 March 2010

Keywords:
Nanocrystalline materials
Mechanical properties
Ni–Co alloy
Microstructure

ABSTRACT

A nanocrystalline (nc) Ni–49.2 mass% Co alloy with an average grain size of 15 nm was synthesized by electrodeposition. Uniaxial tensile tests performed at room temperature and different strain rate showed that the nc Ni–Co alloy exhibits high strength of 1920–2250 MPa and enhanced ductility of 10–13%. The grain refinement, solid-solution hardening and decrease of stacking fault energy, which are caused by alloying of Co element, should be responsible for the excellent mechanical performance. It was deduced from the high strain-rate sensitivity and apparent activation volume that dislocation activity is the dominant deformation mechanism although grain boundary activity may be expected in this alloy.

1. Introduction

It is well known that nanocrystalline (nc) materials with critical grain size usually exhibit the highest strength and hardness, such as 10–20 nm nc Ni [1]. However, their ductility at room temperature (RT) is often disappointingly low compared with their coarse-grained (cg) counterparts [2,3]. The poor ductility of nc materials has become a obstacle for their widespread applications and study of their properties [4]. Most studies about mechanical behaviors of nc materials were carried out mainly using computer simulation techniques [5–7]. Several methods have been applied to improve the ductility of nc materials [4,8], and bulk nc alloy attracted a great deal of attention as potential candidate for next-generation high-strength material. Although improved plastic deformation has been observed in nc Ni–Fe [1,9,10] and Ni–Co [11,12] alloys, the low ductility and deformation mechanism of nc metal with critical grain size is still a problem needed to be substantially resolved. Therefore, it is very necessary to produce suitable samples of fine grain size for mechanical property tests. As to available techniques for fabricating nc metals, electrodeposition is well known as a technological and economical method to produce large scale and high purity nc metals in one step [1,9–14]. In this paper, we fabricated an 15 nm Ni–Co alloy with Co content almost up to 50 mass% by direct-current electrodeposition. The mechanical behaviors of this nc Ni–Co alloy were investigated by uniaxial tensile tests at different strain rates and RT.

2. Experimental procedures

Bulk nc Ni–Co alloy with a thickness of about 350 μm were electrodeposited from an electrolyte containing nickel sulfate, cobalt sulfate, boric acid and some additives at pH level of 5.0 and a temperature of 50 °C. The anode was a pure Ni and the cathode was steel sheet (C1008, AISI). The current density was 2 A/dm^2. The contents of Co and other impurities in the alloy were analyzed by the inductively coupled plasma atomic emission spectrometry (ICP-AES, Plasma/1000). The microstructure was observed by X-ray diffractometer (XRD, D/max 2500PC) and transmission electron microscope (TEM, JEM 2010). Tensile tests were carried out on an MTS-810 system for strain rates ranging from 1.04×10^{-5} to 1.04 s^{-1} at RT, using dog-bone-shaped tensile specimens with 8 mm gauge length and 2.5 mm gauge width. Tensile ductility was measured through the cross-head movement of the tensile machine. Morphologies of the fracture surfaces were observed by scanning electron microscope (SEM, JSM-5600).

3. Results and discussion

The Co content in the Ni–Co alloy was detected to be 49.2 mass% which different from low Co content of previous studies and the main impurities of about 180 ppm S, 300 ppm C, and 100 ppm B. The XRD pattern (Fig. 1) indicates that only face-centered cubic (fcc) phase is observed in the alloy. The positions of the diffraction peaks shift left due to the fcc lattice expansion caused by solid solution of Co in Ni. The ratio of diffraction intensities of (1 1 1)/(2 0 0) is 2.05 indicating the isotropic polycrystalline of this sample. According to the XRD analysis, the average grain size (d) and microstrain of the alloy are 16 nm and 0.343%. The selected area diffraction (SAD) patterns on TEM (Fig. 1 inset) verified the single-phase and fcc structure of the alloy, which is in agreement with the XRD results. Fig. 2(a) displays the TEM bright-field image of the nc Ni–Co alloy. The grains are mostly equiaxed, and no second-phase particles or

* Corresponding author. Fax: +86 431 85095876.
E-mail address: lianjs@jlu.edu.cn (J. Lian).

0925-8388/$ – see front matter © 2010 Elsevier B.V. All rights reserved.
doi:10.1016/j.jallcom.2010.02.139

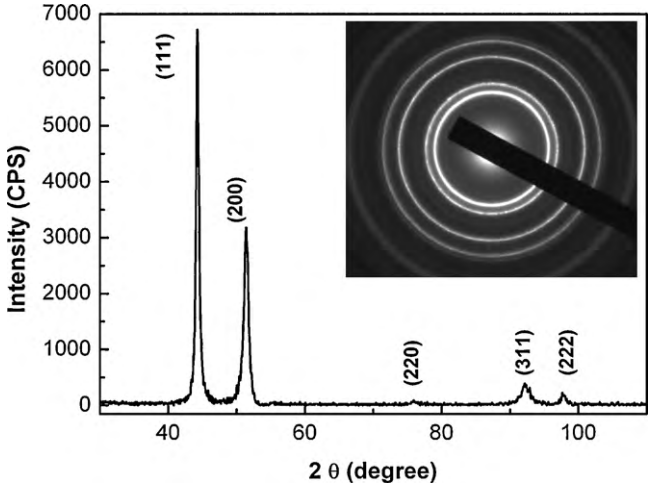

Fig. 1. The X-ray and selected area diffraction (inset) patterns of nc Ni–49.2% Co alloy.

films can be found at the grain boundaries (GBs). The Ni–Co alloy has a narrow grain size distribution according to the grain size distribution plot (Fig. 2(b)) from statistical analysis of about 500 grains. The d of the alloy is 13 nm for number fraction and 17 nm for volume fraction. Therefore, the d of the Ni–Co alloy is determined as 15 nm, close to the result derived from XRD.

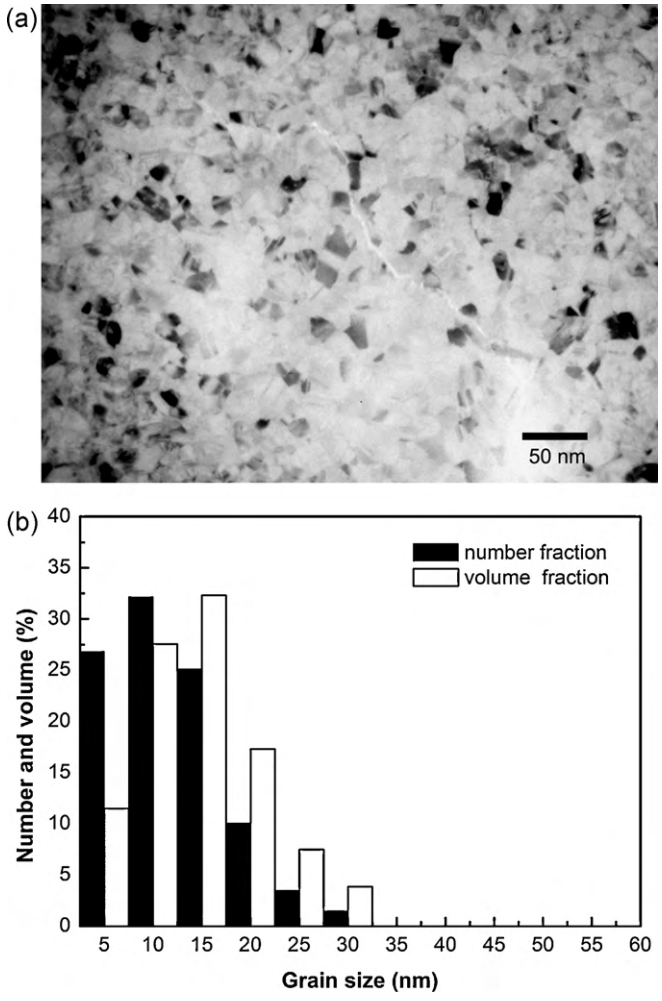

Fig. 2. (a) Bright-field TEM image and (b) grain size distribution plot of the nc Ni–49.2% Co alloy.

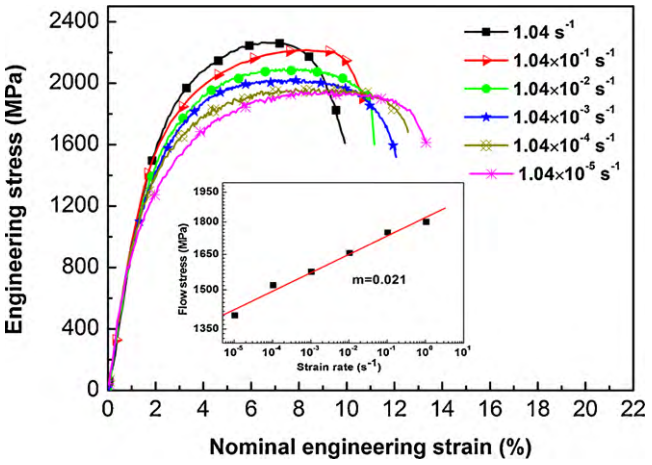

Fig. 3. Nominal engineering stress–strain curves of nc Ni–49.2% Co alloy at different strain rates and RT. The inset is the logarithm plot of flow stress (at 1% plastic strain) versus strain rate. The strain-rate sensitivities value (m) of the nc Ni–49.2% Co alloy is estimated about 0.021.

Fig. 3 presents the nominal engineering stress–strain curves of the nc Ni–Co alloy performed at different strain rate and RT. The ultimate tensile strength (σ_{UTS}) increased from 1920 to 2250 MPa with increasing strain rates, while the elongation to fracture (δ_{ETF}) varies from 13% to 10%. Numerous experimental evidences have shown that nc materials exhibit high strain-rate sensitivity of flow stress, but limited attention was forced on nc alloy [11,13,15]. The strain-rate sensitivity of flow stress is defined as:

$$m = \frac{\partial \ln \sigma}{\partial \ln \dot{\varepsilon}} \tag{1}$$

where σ and $\dot{\varepsilon}$ is flow stress and strain rate, respectively. The flow stress at 1% plastic strain was plotted in logarithmic form as a function of strain rate (Fig. 3(a) inset). The m value measured from the slope is 0.021, which is in the range of 0.02–0.03 for 20 nm Ni [16,17]. The activation volume (V) is widely used recently to determine the possible deformation mechanisms through the tensile test data of nc materials. The experimental activation volume can be given by:

$$V = \sqrt{3}KT\frac{\partial \ln \dot{\varepsilon}}{\partial \sigma} \tag{2}$$

where K is the Boltzmann constant and T is the absolute temperature [18]. The V of the alloy in this study is about $12b^3$, where b is the Burgers vector of Ni. In terms of grain size is about 15 nm, GB-based deformation may be considerable in this alloy [1]. When deformation is controlled by GB activities, V is on the order of b^3–πb^3 [18]. Based on dislocation deformation, many models have been proposed [18–21] to rationalize the relationship between m and V of fcc nc materials. According to the proposed equation [21] to represent the experimental trend of dislocation line length with grain size:

$$L = c \cdot d^{1/2} \tag{3}$$

where c is determined to be 0.98 $nm^{1/2}$ and L is the average dislocation line length which relates to the activation volume by $V = Lb^2$, a larger V of $16b^3$ would be gained for 15 nm Ni–Co alloy. The V of $12b^3$ for the Ni–Co alloy is close to the equation predicted value but little smaller than it. That is to say, single dislocation activity should be the main deformation mechanism, and GB activities would play a minor role during the deformation of this alloy. However, increasing ductility in low strain rate should be attribute to the GBs participate, which relaxes the local stress concentrations and keep sustained work hardening.

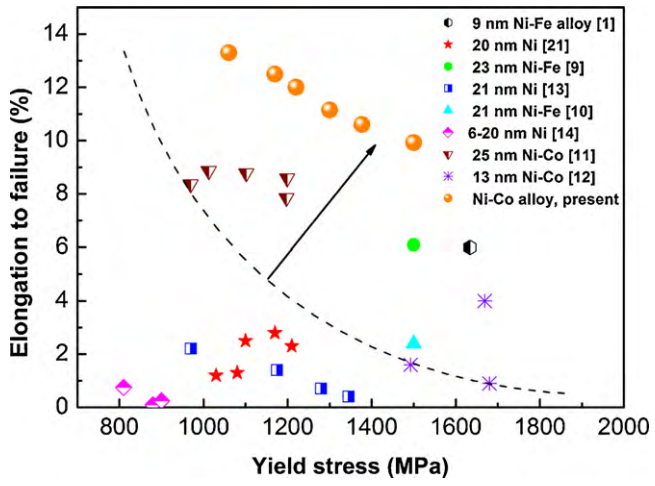

Fig. 4. Summary of elongation to failure vs. yield strength for electrodeposited NC Ni and Ni-based alloys from literatures and present study. The average grain sizes of all samples are smaller than 25 nm.

Fig. 4 summarizes the δ_{ETF} and yield strength for electrodeposited nc Ni and Ni-based alloys from literatures and the present study. The dotted line serves as a guide to distinguish the achieved progress in both high strength and good ductility. It is clearly seen that these reported nc Ni (below dashed line), they exhibit very low δ_{ETF} (less than 3%) and moderate strength (800–1350 MPa). The nc Ni-based alloys (above dashed line) indicate high yield strength and considerably large δ_{ETF}. Because of the smaller grain sizes and shorter gauge length of tensile specimens, Ni–Fe alloy [1,9–10] and Ni–Co alloy [12] show higher strength than present nc Ni–Co alloy. However, the Ni–Co alloy reported by Gu et al. [11] has lower ductility though its grain size are much larger. To the best of our knowledge, there is no report shows δ_{ETF} of nc Ni and Ni-based alloy larger than 10%. Therefore, the present Ni–Co alloy (pointed by black arrow in Fig. 4) is set in the tradeoff region and show a combination of high yield strength and excellent ductility.

The true stress–strain curves of nc Ni–49.2% Co and Ni–8.6% Co [12] alloys at strain rate of $1.04 \times 10^{-3}\,s^{-1}$ and RT are shown in Fig. 5. The inset in Fig. 5 is the variation of normalized work hardening rate (WHR) $[\Theta = 1/\sigma(\partial\sigma/\partial\varepsilon)_i]$ with true strain calculated from the true stress–strain curves. The Ni–49.2% Co alloy shows sustained strain hardening with WHR higher than 1 persisting to about 8%, which would suppress the plastic strain instability and

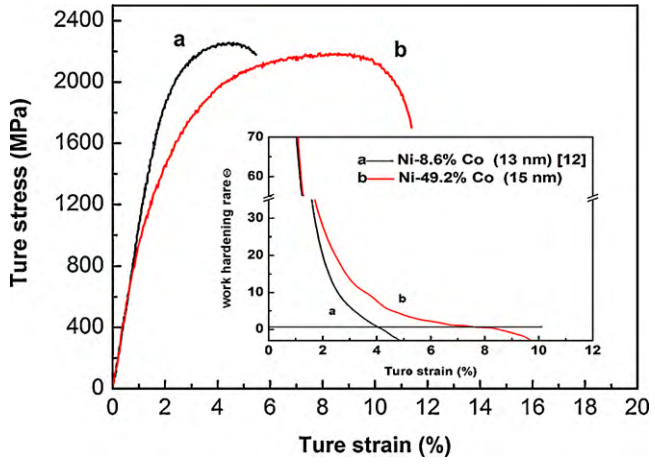

Fig. 5. True stress–strain curves of nc Ni–49.2% Co and Ni–8.6% Co alloys deformed at $1.04 \times 10^{-3}\,s^{-1}$ and RT. The inset is corresponding normalized work hardening rate plotted versus true strain.

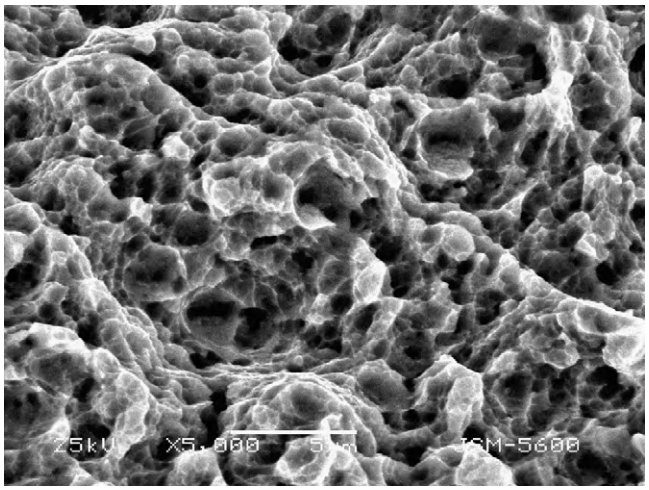

Fig. 6. Fracture morphology of nc Ni–49.2% Co alloy deformed at strain rate of $1.04 \times 10^{-4}\,s^{-1}$ and RT.

improve the ductility of the nc alloy. The high WHR of present nc alloy may come from the solid solution hardening with high content of Co element, which obstructs dislocation motion like that in cg materials. In addition, the lower stacking fault energy (SFE) of nc Ni due to solid solution of Co element will reduce the stress needed to nucleate partial dislocations from GBs and partial dislocation sliding from the GBs is more preferentially [6,22]. So Ni–49.2% Co alloy exhibits a higher strain hardening rate though its grain size is larger. Moreover, a fine grain size (15 nm) and narrow grain size distribution in Ni–49.2% Co alloy leads to high WHR arising from the development of internal stresses due to the strain incompatibility between the presence of finer grains [22,23]. All above factors contribute to the sustained strain hardening which enhances ductility at very high-strength level, and one can deduce that the effect of SFE is more pronounced for materials with smaller grain size as simulation results reported [16].

Typical morphology on fracture surface of nc Ni–49.2% Co alloy is presented in Fig. 6. It shows evident ductile feature with deep dimples structure. The sizes of the dimples are about 500 nm to 1 μm which are several times larger than the grain size (15 nm). Similar dimple-like features have also been observed in other electrodeposited NC materials [11,16], which indicates that the fracture mechanism operates involving collective grain activity. According to molecular dynamic simulation [24], the presence of some special GBs like twin and low-angle GBs are resistant to sliding in the nc structures. The cooperative grain activity leads to the formation of local shear planes concentrated around their neighboring planes and extend over several grain sizes. Therefore, it provides an explanation of the dimension of the dimple structures and some protuberance during the uniform dimples.

4. Conclusion

A bulk 15 nm Ni–49.2 mass% Co alloy was fabricated by a direct-current electrodeposition. The XRD analysis showed the nc Ni–49.2% Co alloy possessed a nearly isotropic polycrystalline fcc structure. The nc Ni–Co alloy shows a high ultimate tensile strength of 1920–2250 MPa and evidently improved tensile ductility to fracture of 10–13% in uniaxial tensile tests at RT. So far, ductility of present Ni–Co alloy is the maximum for reported nc Ni and Ni-based alloy. The combination of excellent strength and ductility is attributed to the grain refinement, solid solution hardening and decrease of stacking fault energy due to solution Co element in Ni crystalline lattice. The measured strain-rate sensitivity ($m = 0.021$) and activation volume ($V = 12b^3$) indicate that dislocation activity

is still the dominant plastic deformation mechanism, although the collaborating GBs activity at low strain rate may enhance the ductility to the higher value of 13%. The significance of present study is that alloying may be a new approach to attain nc materials with both good ductility and high strength.

Acknowledgments

This work was supported by National Nature Science Foundation (Grant No. 50871046) and the Foundation of National Key Basic Research and Development Program (No. 2010CB631001).

References

[1] H.Q. Li, F. Ebrahimi, Appl. Phys. Lett. 84 (2004) 4307.
[2] A. Gouldstone, N. Chollacoop, M. Dao, J. Li, A.M. Minor, Y.L. Shen, Acta Mater. 55 (2007) 4015.
[3] J.R. Weertman, Nanostructured Materials: Processing, Properties and Applications, William Andrews, Norwich, NY, 2002, p. 397.
[4] C.C. Koch, Scripta Mater. 49 (2003) 657.
[5] J. Schiotz, F.D. Di Tolla, K.W. Jacobsen, Nature 391 (1998) 561.
[6] V. Yamakov, D. Wolf, S.R. Phillpot, A.K. Mwkherjee, H. Gleiter, Nat. Mater. 3 (2004) 43.
[7] H. Van Swugenhoven, P.W. Derlet, Phys. Rev. B 64 (2001) 224105.
[8] E. Ma, JOM 58 (2006) 49.
[9] G.J. Fan, L.F. Fu, Y.D. Wang, Y. Ren, H. Choo, P.K. Liaw, G.Y. Wang, N.D. Browning, Appl. Phys. Lett. 89 (2006) 101918.
[10] H.Q. Li, F. Ebrahimi, H. Choo, P.K. Liaw, J. Mater. Sci. 41 (2006) 7636.
[11] C.D. Gu, J.S. Lian, Z.H. Jiang, Adv. Eng. Mater. 8 (2006) 252.
[12] C.D. Gu, J.S. Lian, Q. Jiang, Z.H. Jiang, Mater. Sci. Eng. A 459 (2007) 75.
[13] F. Dalla Torre, H. Van Swygenhoven, M. Victoria, Acta Mater. 50 (2002) 3957.
[14] N. Wang, Z. Wang, K.T. Aust, U. Erb, Mater. Sci. Eng. A 237 (1997) 150.
[15] T. Mukai, S. Suresh, K. Kita, H. Sasaki, N. Kobayashi, K. Higashi, A. Inoue, Acta Mater. 51 (2003) 4197.
[16] K.S. Kumar, H. Van Swygenhoven, S. Suresh, Acta Mater. 51 (2003) 5743.
[17] Y.M. Wang, E. Ma, Appl. Phys. Lett. 85 (2004) 2750.
[18] R.J. Asaro, S. Suresh, Acta Mater. 53 (2005) 3369.
[19] S. Cheng, E. Ma, Y.M. Wang, L.J. Keeskes, K.M. Yousef, C.C. Koch, U.P. Trociewitz, K. Han, Acta Mater. 53 (2005) 1521.
[20] J.S. Lian, C.D. Gu, Q. Jiang, Z.H. Jiang, J. Appl. Phys. 99 (2006) 076103.
[21] C.D. Gu, J.S. Lian, Q. Jiang, W.T. Zheng, J. Phys. D: Appl. Phys. 40 (2007) 7440.
[22] F. Ebrahimi, Z. Ahmed, H.Q. Li, Appl. Phys. Lett. 85 (2004) 3749.
[23] F. Ebrahimi, G.R. Bourne, M.S. Kelly, T.E. Matthews, Nanostruct. Mater. 11 (1999) 343.
[24] A. Hasnaoui, H. Van Swygenhoven, P.M. Derlet, Science 300 (2003) 1550.